Elsevier Editorial System(tm) for Industrial Crops and Products
Manuscript Draft

Manuscript Number:

Title: High surface - highly N-doped carbons from hydrothermally-treated tannin

Article Type: Original Research Paper

Keywords: Hydrothermal carbonisation; Aminated tannin; Nitrogen-doped carbon materials; Carbon gels.

Corresponding Author: Dr. Vanessa Fierro, PhD HDR

Corresponding Author's Institution: CNRS

First Author: Flavia L Braghiroli

Order of Authors: Flavia L Braghiroli; Vanessa Fierro, PhD HDR; Maria T Izquierdo; Julien Parmentier; Antonio Pizzi; Luc Delmotte; Philippe Fioux; Alain Celzard

Abstract: Nitrogen-doped carbon materials (NCMs) were obtained by amination of tannin by hydrothermal carbonisation (HTC). NCMs presented different morphologies depending on the amination method: (i) powders by HTC of tannin in a concentrated aqueous ammonia solution; (ii) gels without using any crosslinker by HTC in distilled water of tannin first dissolved in concentrated ammonia and then evaporated. Whatever the method, (i) or (ii), HTC was carried out at different temperatures: 180, 190, 200, 210 or 220°C, with further pyrolysis at 900°C under nitrogen. The morphology and chemical composition of the resultant materials were discussed. We compared our results with those reported in the open literature and we concluded that HTC of tannin in a concentrated aqueous ammonia solution allowed obtaining outstanding materials because they have both surface areas, higher than 500 m2 g-1, and high N content, around 8 wt.%.

Suggested Reviewers: Guillermo GONZÁLEZ SÁNCHEZ PhD
Senior Researcher, Departamento de Medio Ambiente y Energía, Centro de Investigación en Materiales Avanzados
guillermo.gonzalez@cimav.edu.mx
Specialist in porous materials in general

George Jackson de Moraes Rocha Dr
Senior Researcher, Departamento de Biotecnologia, Escola de Engenharia de Lorena - EEL/USP
george@debiq.eel.usp.br
Specialist in materials derived from biomass

Boris N Kuznetsov Dr
Professor, Siberian Branch of the Russian Academy of Sciences
inm@icct.ru
Specialist in porous materials derived from natural resources

Yoshio Nakano Dr
Tokyo Institute of Technology, Japan
nakano@chemenv.titech.ac.jp

High surface - highly N-doped carbons from hydrothermally-treated tannin

F.L. Braghiroli[1], V. Fierro[*2], M.T. Izquierdo[3], J. Parmentier[4], A. Pizzi[5,6], L. Delmotte[4], P. Fioux[4] A. Celzard[1]

[1]Université de Lorraine, Institut Jean Lamour, UMR 7198, ENSTIB, 27 rue Philippe Séguin, CS60036, 88026 Epinal cedex, France

[2] CNRS, Institut Jean Lamour, UMR 7198, ENSTIB, 27 rue Philippe Séguin, CS60036, 88026 Epinal cedex, France

[3] Instituto de Carboquímica,ICB-CSIC, Miguel Luesma Castán, 4. 50018 Zaragoza, Spain

[4]Université de Haute Alsace, Institut de Science des Matériaux de Mulhouse, UMR CNRS 7361, 15 rue Jean Starcky, BP 2488, 68057 Mulhouse Cedex, France

[5] Université de Lorraine, LERMAB, EA 4370, 27 rue Philippe Séguin, BP 91067, 88051 Epinal cedex 9, France

[6] King Abdulaziz University, Department of Physics, Jeddah, Saudi Arabia

[*]Corresponding author. Tel: + 33 329 29 61 77. Fax: + 33 329 29 61 38. E-mail address : Vanessa.Fierro@univ-lorraine.fr (V. Fierro)

Abstract

Nitrogen-doped carbon materials (NCMs) were obtained by amination of tannin by hydrothermal carbonisation (HTC). NCMs presented different morphologies depending on the amination method: (i) powders by HTC of tannin in a concentrated aqueous ammonia solution; (ii) gels without using any crosslinker by HTC in distilled water of tannin first dissolved in concentrated ammonia and then evaporated. Whatever the method, (i) or (ii), HTC was carried out at different temperatures: 180, 190, 200, 210 or 220°C, with further pyrolysis at 900°C under nitrogen. The morphology and chemical composition of the resultant materials were discussed. We compared our results with those reported in the open literature and we concluded that HTC of tannin in a concentrated aqueous ammonia solution allowed obtaining outstanding materials because they have both surface areas, higher than 500 m^2 g^{-1}, and high N content, around 8 wt.%.

Keywords: Hydrothermal carbonisation; Aminated tannin; Nitrogen-doped carbon materials; Carbon gels

1. Introduction

N-doped carbon materials (NCMs) have gained an increasing interest in the last decade, mainly because doping carbonaceous materials with nitrogen is an effective way of modifying their surface chemistry and improving their electrochemical properties(Lee et al., 2011; Nieto-Marquezet al., 2009).It has been suggested that NCMs provide pseudocapacitance through pseudofaradaic reactions and also enhance the electronic conductivity of carbon structures. For these reasons, such kind of materials can be used in electric double-layer capacitors (Frackowiak et al., 2006; Hulicova et al., 2006; Hulicova-Jurcakova et al., 2009) and also in fuel cells (Qiu et al., 2011; Steele and Heinzel, 2001).NCMs can also act as efficient adsorbents of SO_2 from flue gases, or of phenol from aqueous effluents (Bimer et al., 1998; Li et al., 2001; Przepiórski, 2006).

NCMs can be obtained from biomaterials naturally containing high levels of nitrogen or from chemically modified carbons (Bimer et al., 1998). A recent work has shown that NCMs can successfully be prepared from an abundant biomaterial, tannin, submitted to hydrothermal carbonization (HTC) in a concentrated ammonia solution at 180°C, followed by pyrolysis at 900°C (Braghiroli et al., 2012). The structure of the main compound contained in condensed Mimosa tannin extract (*Acacia mearnsii*, de Wild) is presented in Fig. 1. Mimosa tannin is a suitable product for preparing carbonaceous materials, as it is based on phenolic molecules and contains aromatic structures such as resorcinol, pyrogallol and catechol. Such tannin is quite reactive and can be extracted from several species of *Acacia* trees (Pizzi, 2008; Pizzi and Mittal, 2003).The corresponding condensed polyflavonoid species comprise flavan-3-ols having approximately 70% of repeating units of robinetinidin (resorcinol A-ring; pyrogallol B-ring), which is shown in Fig. 1, and 25% of fisetinidin (resorcinol A-ring; catechol B-ring)(Bate-Smith and Swain, 1962;Hemingway, 1989; Pizzi, 1983; Pizzi, 1994). Moreover, it has been also proved that tannin, in the presence of a crosslinker such as formaldehyde,

hexamethylenetetramine, glyoxal, or 1-, 3-, or 5-trioxane, is a very suitable material for preparing high-quality and low-cost gels and related carbon materials. Mimosa tannin is thus able to replace resorcinol, which is the standard reagent used to prepare the same kind of materials (Amaral-Labat et al., 2012; Amaral-Labat et al., 2013b; Braghiroli et al., 2013; Grishechko et al., 2013; Reddy et al., 2003).

Amination is an easy way of incorporating nitrogen into phenolic compounds. Until recently, amination of Mimosa tannin was thought to be regioselective, only affecting the position 4' at which the hydroxyl group can be converted into amine (see asterisk in Fig. 1) (Hashida et al., 2009). However, we have recently demonstrated that reactions of flavonoid tannins in concentrated ammonia solution at room temperature are more complex, leading to multiamination of a higher proportion of phenolic hydroxyl groups in both A and B rings, as suggested in Fig. 1, also possibly opening the heterocycle as well as producing oligomerisation and crosslinking between flavonoid units through –N= bridges (Braghiroli et al., 2013). Surface areas as high as 500 m^2 g^{-1}, and nitrogen content as high as 6.3 wt. %, were obtained, depending on the amination method (Braghiroli et al., 2012). However, both high surface area and high nitrogen content could not be obtained simultaneously in the same material, the one having the highest N content being the one having the lowest surface area, and vice versa. The need of meeting the desirable target of having both high N content and high surface area motivated the present study.

Therein, monolithic NCMs gels and NCMs powders were prepared by HTC of tannin in the absence of crosslinker. We show here that, in hot pressurised water at a temperature within the range 180 – 220°C, HTC is a powerful way of preparing N-doped carbonaceous materials from flavonoid tannin, presenting nitrogen contents up to 13.7 and 8.1 wt.% before and after pyrolysis at 900°C, respectively.

2. Experimental

2.1 Materials

2.1.1 *Tannin*

Commercial Mimosa tannin, extracted industrially in Tanzania, was kindly supplied by the company SilvaChimica (Italy). The procedure, based on leaching Mimosa barks with a warm aqueous solution, has been detailed elsewhere (Amaral-Labat et al., 2013a). The resultant tannin solution was then concentrated and spray-dried, leading to a light-brown powder containing 80 – 82% of actual phenolic flavonoid materials, 4 – 6% of water, 1% of amino and imino acids, the remainder being monomeric and oligomeric carbohydrates, in general broken pieces of hemicelluloses.

2.1.2 *Amination and HTC*

Aminated tannin samples were prepared by dissolving 2.0 g of raw tannin powder in 16 mL of a 28-30 wt.% of ammonia in water. Two different procedures were carried out. In the first one, leading to samples called H-AT (hydrothermal-aminated tannin), the tannin solution in ammonia was directly submitted to HTC. In the second one, the same mixture was evaporated at room temperature, and then the resultant powder was submitted to HTC in distilled water, leading to samples called H-EAT (hydrothermal-evaporated aminated tannin). A control sample called H-T (hydrothermal-tannin) was also prepared for comparison purposes, using the same amount of tannin: 2.0 g in 16 mL of water.

Both methods have been already described in detail elsewhere (Braghiroli et al., 2012). Each tannin solution was put in an open glass vial, itself placed into a Teflon-lined autoclave for HTC. The autoclave, always filled at one third of its available inner volume whatever the sample, was closed and placed into a pre-heated ventilated oven for 24 h at different temperatures, between 180 and 220°C. After HTC, the autoclave was left to cool down atroom

temperature. The resultant dark powders or monoliths, depending on the synthesis method, were recovered, washed with distilled water and then placed inside of a vacuum oven at 80°C for drying during 12h.

2.1.3 *Pyrolysis*

Pyrolysis was carried out under nitrogen flow in a tubular furnace at a heating rate of 1°C min^{-1} up to 900°C, and the final temperature was maintained for 3 hours. Pyrolysed H-T, H-EAT and H-AT samples were labelled CH-T, CH-EAT and CH-AT, respectively.

2.2 Characterisation

2.2.1 *NMR and MALDI-ToF studies*

Solid-state CP-MAS (cross-polarisation/magic angle spinning) ^{13}C NMR spectra for H-T, H-AT and H-EAT were recorded on a Bruker MSL 300 FT-spectrometer at a frequency of 75.47 MHz. Chemical shifts were calculated with respect to tetramethylsilane (TMS). The rotor was spun at 4 kHz on a double-bearing 7 mm Bruker probe. The spectra were acquired with 5 s recycle delays, a 90° pulse of 5 μs and a contact time of 1 ms. The number of transients was 3000, and the decoupling field was 59.5 kHz.

MALDI-ToF (Matrix-Assisted Laser Desorption Ionisation – Time of Flight) spectra were recorded on a Shimadzu Axima Precision instrument. 5 mg of each sample were dissolved in 1 mL of an aqueous solution acetone:water (1:1), and then mixed with a matrix, 2,5-dihydroxy benzoic acid/tetrahydrofuran. For the enhancement of ion formation, NaCl was added to the matrix. The resulting solution was placed on the MALDI target. After evaporation of the solvent, the MALDI target was introduced into the spectrometer. The irradiation source was a pulsed nitrogen laser with a wavelength of 337 nm. The length of one laser pulse was 3 ns. The measurements were carried out using the following conditions: polarity-positive, flight

path-linear, mass-high (20 kV acceleration voltage), 100 – 150 pulses per spectrum. The delayed extraction technique was used applying delay times of 200 – 800 ns.

2.2.2 *Elemental analysis*

Bulk elemental analyses were carried out in a ThermoFlash 1112 apparatus to determine carbon, hydrogen, nitrogen and sulphur contents. Oxygen content was obtained by difference. Surface elemental analyses were performed by X-ray photoelectron spectroscopy (XPS), using an ESCAPlus OMICROM system equipped with a hemispherical electron energy analyzer. The spectrometer was operated at 10 kV and 15 mA, using a non-monochromatized Mg Kα X-ray source (hν = 1253.6 eV) under vacuum (< 5 × 10-9 Torr). Analyzer pass energy of 50 eV was used for survey scans and 20 eV for detailed scans. The C1s peak around 284.5 eV was used for binding energy correction. A survey scan (1 sweep/200 ms dwell) was acquired between 1100 and 0 eV. Current region sweeps for N1s, O1s and C1s were obtained. The CASA data processing software allowed smoothing, Shirley-type background subtraction, peak fitting and quantification.

2.2.3 *Morphology and texture*

Samples' morphology was observed with a FEI Quanta 400 scanning electron microscope (SEM). Pore texture parameters were derived from nitrogen or krypton adsorption isotherms at -196°C using a Micromeritics ASAP 2020 automatic apparatus, whether they were determined before or after pyrolysis at 900°C, respectively. The choice of the probe molecule was dictated by the surface area, which was very low for non-pyrolysed samples, and for which Kr adsorption was thus much more accurate. Prior to any adsorption experiment, non-pyrolysed and pyrolysed samples were degassed for 48 h under vacuum at 60°C or at 250°C, respectively. Kr and N_2 adsorption studies were carried out, and the corresponding isotherms were treated for obtaining the texture parameters. From N_2 adsorption isotherms, the following

quantities were obtained: surface area (S_{BET}), from the BET calculation method (Brunauer et al., 1938) in the 0.01 to 0.05 P/P_0 interval, micropore volume (V_μ) (Dubinin, 1989); total pore volume ($V_{0.97}$)determined as the N_2 adsorbed at P/P_0 = 0.97;and mesopore volume (V_m), calculated as the difference $V_{0.97}$– V_μ (Gregg and Sing, 1991). From Kr adsorption isotherms, the surface area (S_{BET}) was obtained in the 0.05 to 0.2 P/P_0 interval.

3. Results and discussion

3.1 Chemical structure of hydrothermally treated tannin

Solid-state ^{13}C NMR spectra of hydrothermal carbons H-T, H-EAT and H-AT, obtained after HTC at 180°C, are shown in Fig. S1 of Supplementary Material. The detailed interpretation of these spectra is also given in Supplementary Material, but the main conclusions are the following. H-T has a similar structure as that of flavonoid tannin, but presents a much higher level of polymerisation, mainly through the opening of the heterocyclic C2–ring and subsequent partial condensation between C2 (open) to C6 or C8, and partly through some autocondensation C4 to C6 and C8. H-EAT shares the main features of H-T in terms of autocondensation and heterocyclic C2-ring opening, but is also characterized by the amination of C3' and C4' sites, the preservation of some heterocyclic structures, and a lower level of polymerization. The presence of –NH– bridges is also observed, possibly explaining why H-EAT is a gel whereas no crosslinker was initially present in the system. Finally, H-AT is a highly polymerized and crosslinked material, in which the typical tannin structure is almost completely lost.

MALDI-ToF spectra of the same materials and their detailed interpretation are given in Fig. S2 of Supplementary Material. H-T, although polymerised as proved by NMR spectra, exhibits the classical features of normal tannin, as the expected flavonoid units are detected.

H-EAT, as a gel, is totally different, and the long three-dimensional chains from which it is made cannot be detected with this technique. The few peaks of the spectrum were attributed to flavonoid structures doped by nitrogen, such as those shown in Fig. 2(a-b), accounting for the observed peaks at 554 and 555 Da. As the $–NH_2$ groups can have substituted any one of the –OHs of the two flavonoid units from which these species are based on, their distribution is likely to be variable. A small peak at 843-844 Da was interpreted as shown in Fig. 2(c), i.e. by a 554 or 555 Da compound above to which has been added a 290-1 = 289 Da unit, either a robinetinidin or a catechin. Finally, H-AT presents many species in which –OH groups have been substituted by $–NH_2$ groups. More details are given in Supplementary Material.

3.2 Elemental composition of all materials

The elemental analyses of all materials prepared by HTC at different temperatures: 180, 190, 200, 210 and 220°C are given in Table S3 of Supplementary Material, before and after pyrolysis at 900°C. The carbon content slightly increased with HTC temperature, whatever the preparation method. This finding was observed at the same small extent after pyrolysis at 900°C. The carbon content of natural tannin mimosa extract used in this work was 53.8 wt.%, and only increased by 5-11% after HTC. Whereas such kind of material is unanimously called "hydrothermal carbon" in the literature (Baccile et al., 2009), the resultant microspheres or gels are thus not really carbon materials until a pyrolysis is carried out at much higher temperature. Indeed, and as shown in Table S3, the carbon content reached around 90 wt.% after pyrolysis.

Fig. 3 shows nitrogen content for materials before and after pyrolysis. Tannin contains naturally nitrogen due to the presence of amino and imino acids. H-T materials had nitrogen content lower than 1%, which still decreased after pyrolysis. As expected, pyrolysis at 900°C produced a significant decrease of the nitrogen content. Nitrogen is indeed a volatile element, which evolves as more easily as the heat-treatment temperature and/or the porosity of the

material in which it is contained is high. The challenge was thus to prepare materials having both a high porosity and a high nitrogen content. H-EAT materials, having a nitrogen content around 4 wt.%, led to materials, CH-EAT, whose N content was close to 2 wt.% after pyrolysis, irrespective to the HTC temperature as a first approximation. In contrast, increasing HTC temperature produced a nitrogen enrichment of H-AT materials, with an outstanding N content ranging from 12 to 14 wt.%. After pyrolysis, a roughly constant but still amazing 8 wt.%, on average, was obtained in CH-AT materials.

The percentage of nitrogen after amination of tannin would have been 4.8 wt.% if only the site 4' of the B-ring (see again Fig. 1) was aminated, which situation happens at room conditions according to Hashida et al. (2009) and Morisada et al. (2011).This statement is consistent with the results for H-EAT. However, as recently shown Braghiroli et al. (2013)and again suggested by the present NMR and MALDI-ToF spectra, tannin can be aminated on both A and B rings, and can also bear –N= bridges between flavonoid units as seen in Fig. 1, thereby justifying higher nitrogen contents. However, for the sample having the highest N content, H-AT, the NMR spectrum was hardly interpreted and the MALDI-ToF studies did not help much, as $–NH_2$ and –OH have very close molecular weights, and cannot be separated in oligomers prone to be partly deprotonated. The molecular structure of N-doped tannin after direct HTC in concentrated ammonia is still unknown, but should explain so high nitrogen contents ranging from 11 to 13 wt.% before pyrolysis. Our previous characterizations of this kind of materials by XPS showed that H-EAT had a higher content of N-6 than H-AT, the remainder being neutral amines. After pyrolysis at 900°C, the amount of N-6 decreased, and N-5, N-X and maybe some N-Q were formed, but the corresponding moieties were the same in both CH-EAT and CH-AT (Braghiroli et al., 2012).

Nitrogen-doped carbon materials were also prepared by HTC of chitosan and subsequent pyrolysis at 750°C, having carbon and nitrogen contents of 79.2 wt.% and around 9.0

242 wt.%,respectively (Zhao et al., 2010a). The same method applied to glucosamine led to C and
243 N contents of 81.6 and 6.6 wt.%, respectively (Zhao et al., 2010a). Such N contents are similar
244 or below those measured in CH-AT, despite the significantly lower temperature of pyrolysis,
245 750°C, in favour of a much lower loss of nitrogen during the heat treatment. Zhang et al.
246 (2012)studied the amination of sucrose by HTC in ammonia at 160, 180 and 200°C, followed
247 by pyrolysis at 900°C. The resultant materials can thus be compared to H-AT and CH-AT and
248 their C and N contents were around 64 and 20 wt.% before pyrolysis, respectively, and 94.8
249 and 4.4 wt.% after pyrolysis, respectively. Reaching around 8 wt.% of nitrogen in CH-AT
250 even after heat-treatment at 900°C suggests that nitrogen was well stabilised in the
251 carbonaceous structure.
252 3.3 XPS analysis
253 The chemical analysis of the surface of the aminated tannin (EAT), dried hydrogels (H-
254 AT, H-EAT) and carbon gels (CH-AT, CH-EAT) was investigated by XPS. XPS spectra of N-
255 doped materials, with emphasis on the energy range corresponding to N1s are given in Fig. S3
256 of Supplementary Information part, with the corresponding curve fits allowing the
257 deconvolution of the peaks. The corresponding data are given in Tables 1 and 2. Caution
258 should be taken regarding the assignment of XPS peaks to chemical groups since the low
259 abundance of N increases the uncertainty of the multi-component curve-fitting peak and, non-
260 conductive samples (EAT, H-AT and H-EAT) could lead to local charging effect with shifted
261 binding energy to higher values. Moreover, the assignment is complicated by the location of N
262 within the polyaromatic network and the degree of condensation of the graphene layer
263 (Lahaye et al., 1999). For instance, N in pyridinic groups has its core level binding energy that
264 lie from 398.3 eV for conducting samples (e.g. N-doped graphite) up to 399.3 eV for isolated
265 pyridine group within the non-conducting poly(2-vinylpyridine) polymers or pyridinic N
266 located in a border of a polyaromatic cycle. A common way to assign peaks and especially N

in pyridinic group is to determine the energy difference $\Delta|N1s - C1s|$ between the binding energy of N1s and reference C1s taken at the maximum of the C1s envelope for C-C or C=C bonds. For different reference compounds containing pyridinic N, Δ values range from 113.7 to 114.3 eV (Lahaye et al., 1999). Assignment of other peaks could then be done by the relative shift to that N-pyridinic reference.

For tannin modified with ammonia at room temperature (EAT), XPS composition reveals a high fraction of O (28 at.%), a minor amount of N (3 at.%) and traces of K (0.65 at.%). The N1s peak exhibits two components at 399.9 and 402.1 eV. Based on the previous discussion, $\Delta|N1s - C1s|$ was calculated with the binding energy of 399.9 eV and 284.7 eV for N1s and C1s respectively. It leads to a value of 115.2 eV, outside the range of 113.7 to 114.3 eV expected for N pyridine species (Lahaye et al., 1999). It suggests that the main peak at 399.9 eV could not be attributed to pyridinic N species but rather to functional groups having slightly higher binding energy, around + 1.1 eV with respect to the averaged N pyridinic binding energy (398.8±0.5 eV). This feature is in agreement with our previous study of EAT using Maldi-Tof and solid NMR spectroscopies where no pyridinic groups were detected (Braghiroli et al., 2013). Moreover, it is well known in the literature that conversion of carbonaceous materials containing no pyridinic groups (e.g cellulose) to pyridinic nucleiis supposed to occur at temperature higher than 250°C in presence of gaseous NH_3 (Cagniant et al., 2002). Therefore, the possible N-containing chemical groups are attributed mainly to neutral amine and/or amide since both functions could have their binding energy in the range around 399.9 eV. Regarding imine groups, only traces could be present if we consider their classical binding energy around 398.5 eV. They could more significantly be present by considering their assignment at 399.0 ±0.1 eV as performed by Cagniant et al. (2002) by coupling XPS and IR spectroscopies for ammonia-treated cellulose at low temperature (250°C). In that case, these data appear in agreement with the previous characterization of

EAT (Braghiroli et al., 2013) where multiamination of phenolic hydroxyl groups with formation of bridging -C=N- group and oxidation of phenolic-OH groups to quinone were observed. The latter point could explain the high oxygen content determined by XPS at the surface of the sample. The peak at 402.1 eV was attributed to quaternary nitrogen such as protonated amides or amines.

When tannin and EAT were submitted to hydrothermal treatment in concentrated aqueous ammonia (H-AT) or in water (H-EAT) respectively, the XPS compositions evolve as shown in Table 2, with a decrease of the oxygen content in both cases and a significant nitrogen enrichment, around 3 at% for H-EAT up to 8-9 at% for H-AT compared to 0.6 at% for natural tannin and 1 at% after HTC of tannin. Presence of Si (0.7 at % for H-EAT) could also be detected when silica vials were used in the autoclave during HTC.

Based on the literature, the presence of pyridinic species is now possible since it is well know that HT process promotes the carbonisation of tannin with polycondensation of aromatic units and formation of N-containing cycles such as pyridinic species (Baccile et al., 2011; Wohlgemuth et al. 2012a; Wohlgemuth et al., 2012b). For instance, Cagniant et al. (2002), have proposed the formation of pyridinic group during the carbonization of cellulose at 250°C in ammonia atmosphere (Cagniant et al., 2002). The N1s XPS spectra shown an asymmetry of the main peak associated with a shift to lower binding energy compared to EAT sample (399.3-eV instead of 399.9 eV). The $\Delta|N1s - C1s|$ values were around 114.8 eV, outside the expected range for pyridinic species, suggesting that the N- pyridinic species are not the main contribution to this peak. Indeed, its presence could not be excluded since the N1s binding energy domains of pyridinic groups are scattered in a large range (1eV). The latter overlap those of neutral amines and therefore, the asymmetric N1s peaks were assigned to these two species without any possible deconvolution of individual contributions as mistakenly done in our previous study (Braghiroli et al., 2012).

After carbonization at 900°C, no amines were present, as expected, and they were mainly replaced by pyridinic N-6 and to a lower other species such as pyrrolic (N-5) or pyridonic (not distinguishable by XPS measurements), quaternary pyridinic nitrogen (N-Q) (Lahaye et al., 1999) or pyridine oxide groups. Despite the high purity of the inert gases used for carbonization, the presence of oxide forms (pyridone, pyridine oxide) could be ascribed to the reactivity of carbonized materials with air as previously observed in the works of Pels et al. (1995) and Lahaye et al. (1999).

3.4 Materials' morphology and porous texture

Figure 4 shows materials morphology for samples prepared at 190 and 210°C. CH-T materials are spherical particles, more or less connected with each other, whose average diameter and agglomeration state increased with HTC temperature (Fig. 4(a-b)). The same was observed for the material directly aminated at HTC conditions, CH-AT (Fig. 4(c-d)), but the polydispersity was much higher at 210°C. Indeed, whereas the particles were rather monodisperse at 190°C, a mixture of small and very big particles was found after HTC at 210°C. Fig. 4(d) even shows big, basketball-like, spheres. CH-EAT (Fig. 4(e-f)) is a carbon gel within which the spherical nodules were so small that they were hardly observed at the magnifications used. CH-EAT is in fact a carbon xerogel as the material was dried in vacuum at 80°C before pyrolysis at 900°C. Fig. 4(f) also shows that bigger particles with a higher polydispersity were obtained with increasing temperature. Li et al. (2011) submitted glucose to HTC and also found that the most spherical particles were formed at lower temperatures of 180-190°C, whereas more polydisperse spheres with broken shapes appeared at higher temperatures such as 210°C. On the contrary, Titirici et al. (2013) found that higher temperatures led to larger but more homogeneous particles when glucose was submitted to HTC at temperatures from 120 to 280°C.

Although comparisons are made all along the present paper with materials derived from HTC of polysaccharides, for which the literature is the most abundant, tannin treated in similar conditions behaves differently in some aspects. For example, amino-functionalised materials prepared by HTC of glucose in ammonia at pH 11 at 150°C were obtained in the form of spheres having a very narrow distribution of diameters centred on around 2-3 μm (Wang et al., 2012). In the case of tannin, the best, most spherical particles were obtained at 180 – 190°C, lower temperatures within the range 130 – 160°C leading to much more irregular and polydisperse spheres (Braghiroli et al., 2014).

Fig. 5 shows the specific surface areas of all materials prepared at different HTC temperatures, measured before and after pyrolysis at 900°C. Before pyrolysis, the gel H-EAT was the material having the highest surface area, around 100 m^2 g^{-1}. This is a logical result, considering that such material comprises the smallest particles. In contrast, H-T was the one having the lowest surface area, less than 1 m^2 g^{-1}, due to his rather monodisperse, solid and big, spherical particles. As expected, H-AT had values of surface area between those of the former two materials, slightly lower than 20 m^2 g^{-1}, since its morphology is in-between a powder and a gel. All the materials had surface areas that decreased slightly when the HTC temperature increased, due to both growth and agglomeration of the particles. The effect was the most significant in the case of H-EAT, whose very small nodules were more affected by particle growth and Ostwald ripening.

After pyrolysis at 900°C, the materials CH-T, CH-AT and CH-EAT presented developed porosity and significantly higher surface areas, as shown in Fig. 5. Depending on the preparation method, different effects of the HTC temperature were observed. CH-T presented the highest surfaces areas, around 670 m^2 g^{-1}, which did not change much when the HTC temperature increased. Such values are higher than most results reported so far for carbohydrates submitted to HTC and subsequently pyrolysed at high temperature. Glucose,

366 chitosan and glucosamine indeed presented low porosity not only after HTC, but also after
367 pyrolysis, so that the resultant measured surface areas were around 30-50 m^2 g^{-1} in general
368 (Zhao et al., 2010a). In the case of CH-AT, the materials obtained by HTC at 185-190°C and
369 subsequent pyrolysis had the highest value of surface area, up to 550 m^2 g^{-1}. Higher HTC
370 temperatures led to lower surface areas probably due to the formation of bigger and less
371 porous carbon spheres, as suggested by Fig. 4(d). The surface areas of the carbon gel CH-EAT
372 presented a maximum at 180°C, the lowest HTC temperature. On average, the surface area of
373 CH-EAT was around 400 m^2 g^{-1}.

374 Fig. 6 shows the nitrogen adsorption-desorption isotherms at -196°C for the materials
375 shown in Fig. 4. Nitrogen adsorption isotherms of CH-T materials were type I, according to
376 the IUPAC classification, with a sharp increase of the nitrogen amount adsorbed at P/P_0 lower
377 than 0.05, a narrow knee and a plateau up to P/P_0 equal to 0.99. These isotherms are
378 characteristic of purely microporous solids. Nitrogen adsorption isotherms of CH-AT
379 materials were similar to those of CH-T but presented a lower volume adsorbed at low $P/P_0 <$
380 0.05, indicating a lower microporosity than CH-T materials, and a sudden increase of the
381 nitrogen uptake $P/P_0 < 0.95$, indicating capillary condensation in wide mesopores. Nitrogen
382 adsorption isotherms of CH-EAT materials were combinations of types I and IV, for which
383 adsorption of nitrogen takes place in both micro and mesopores. The existence of a well-
384 developed mesoporosity is also indicated by the slope of the adsoption isotherms, in the P/P_0
385 range from 0.05 to 0.7, and by the large hysteresis cycle. Textural parameters of all the carbon
386 materials prepared are given in Table S4.

387 The carbon xerogels, CH-EAT materials, were those materials presenting the highest
388 proportion of mesopores, between 66 and 76% of the total pore volume. Whereas these
389 materials were xerogels, i.e. were not submitted to supercritical drying after synthesis, a
390 significant amount of mesoporosity was thus maintained. N-doped carbon materials were also

prepared by White RJ et al. (2011) from the HTC of glucose and ovalbumin. A gel was obtained, which was dried by exchange with supercritical CO_2, and then pyrolysed. The resultant carbon aerogel also presented a high mesopore volume of 0.51 cm^3 g^{-1}, and its surface area was 310 m^2 g^{-1}. These characteristics are thus similar to those of our CH-EAT_200°C sample, but in our case a simple subcritical drying was carried out. Therefore, our process is expected to be much more convenient and cheaper for preparing N-doped porous carbon materials.

3.4 Comparison with other N-doped carbon materials

Fig. 7(a) gathers the data of surface area and nitrogen content of all the tannin-derived materials prepared by HTC in the present work. The same kind of data is also given on the same plot for other carbonaceous materials produced by HTC of various precursors, such as chitosan, glucose and glucosamine (Zhao et al., 2010a), glucose and albumin (Baccile et al., 2010), glucose and ovalbumin (White et al., 2011) and D-glucosamine (Zhao et al., 2010b). H-T presented both low surface area and very low nitrogen content, but their aminated counterparts were among the materials having either the highest N content (H-AT) or the highest surface area (H-EAT). But none presented both high characteristics at the same time. The H-EAT gel was comparable to the material obtained by HTC of a mixture of glucose and albumin (Baccile et al., 2010), having values of S_{BET} and N content around 100 m^2 g^{-1} and 4-5 wt.%, respectively. Fig. 7(b) shows results for the same precursors as in Fig. 7(a) and a few others more, such as cystine and T-cystine (Wohlgemuth et al., 2012b) and prawn shells (White et al., 2009) after HTC and posterior pyrolysis at different temperatures: 550 (Wohlgemuth et al., 2012b), 750 (Baccile et al., 2010; White et al., 2009; White et al., 2011;Zhao et al., 2010a), 900 (Wohlgemuth et al., 2012b) and 950°C (Baccile et al., 2010; White et al., 2011). After KOH activation at 600°C of D-glucosamine submitted to HTC (Zhao et al., 2010b), S_{BET} as high as 600 m^2g^{-1} was obtained but N content was only 2.3

wt.%.Even higherS_{BET}, 730 m^2g^{-1}, was obtained after carbonisation at 900°C of T-cystine submitted to HTC but N content was lower than 4 wt.% (Wohlgemuth et al., 2012b). Pyrolysis obviously led to a significant decrease of nitrogen content, and especially at the highest temperatures. However, it is important to point out that despite H-AT was heat-treated at 900°C, the resultant carbon CH-AT was among the materials presenting the highest N content, around 8 wt.%, with a surface area as high as 500 m^2g^{-1}.

In this study, we obtained carbon materials with simultaneously high nitrogen content and high surface areas. Specially tannin directly submitted to HTC in concentrated ammonia at 190°C and pyrolysed at 900°C presented S_{BET} and nitrogen content of 500 m^2 g^{-1} and 8 wt.%, respectively. The incorporation of nitrogen in the carbonaceous structure is indeed expected to increase its electrical conductivity and provide pseudofaradaic reactions, thus further increasing the capacitance and the performances of the porous electrode. Therefore, this material is foreseen to be tested in several applications, in particular as electrode of electric double-layer capacitor. This will be done in the near future.

4. Conclusion

Hydrothermal carbonisation (HTC) has been used to produce carbonaceous materials from Mimosa tannin in water or in 28 – 30 wt.% ammonia solution, and at temperatures ranging from 180 to 220°C. N-doped materials were obtained either by tannin amination in ammonia in room conditions followed by HTC in distilled water (H-EAT), or by direct HTC in ammonia (H-AT). The former method led to gels despite no crosslinker was present, and the latter led to microspheres. All were based on autocondensed and partly dehydrated tannin, mainly through heterocycle opening, the level of polymerisation depending on the preparation method. The N-doped materials presented rather low surface areas, but H-AT had outstanding nitrogen contents as high as almost 14 wt.%. Most of the nitrogen was in the form of amines,

with some possible pyridinic N. MALDI-ToF and NMR studies proved that nitrogen was incorporated at several sites of the flavonoid units, unlike previous studies indicated.

Pyrolysis at 900°C systematically decreased the N content, as expected given the volatility of this element, but simultaneously led to a significant porosity development. As a consequence, the CH-AT material prepared by HTC at 190°C presented high surface area and high N content, 500 m^2 g^{-1} and 8 wt.%, respectively. To our deepest knowledge and after having extensively revised the open literature, no other natural precursor submitted to HTC reached so high N content and so high surface area at the same time. Such N-doped carbons, prepared by a cheap and sustainable method, are very promising materials in a broad range of applications such as water purification and electrochemical energy storage and conversion, amongst others. These applications are presently under study.

Acknowledgements

The present research was partly made possible by the support of the Region Lorraine and UHP through the programme 'Jeunes chercheurs'. The French authors from laboratories hosted by ENSTIB also gratefully acknowledge the financial support of the CPER 2007-2013 "Structuration du Pôle de Compétitivité Fibres Grand'Est" (Competitiveness Fibre Cluster), through local (Conseil Général des Vosges), regional (Région Lorraine), national (DRRT and FNADT) and European (FEDER) funds.

References

Amaral-Labat, G., Grishechko, L.I., Szczurek, A., Fierro, V., Pizzi, A., Kuznetsov, B.N., Celzard, A., 2012. Highly mesoporous organic aerogels derived from soy and tannin. Green Chem. 14, 3099-3106.

Amaral-Labat, G., Grishechko, L.I., Fierro, V., Kuznetsov, B.N., Pizzi, A., Celzard, A., 2013a. Tannin-based xerogels with distinctive porous structures. Biomass Bioenergy 56, 437-445.

Amaral-Labat, G., Szczurek, A., Fierro, V., Pizzi A., Celzard, A., 2013b. Systematic studies of tannin – formaldehyde aerogels: preparation and properties. Sci. Technol. Adv. Mater. 14, 1-13.

Baccile, N., Laurent, G., Babonneau, F., Fayon, F., Titirici, M.M., Antonietti, M., 2009. Structural characterisation of hydrothermal carbon spheres by advanced solid-state MAS ^{13}C NMR investigations. J. Phys. Chem. C 113, 9644-9654.

Baccile, N., Antonietti, M., Titirici, M.M., 2010. One-step hydrothermal synthesis of nitrogen-doped nanocarbons: albumine directing the carbonization of glucose. ChemSusChem 3, 246–253.

Baccile, N., Laurent, G., Coelho, C., Babonneau, F., Zhao, L., Titirici, M.M., 2011. Structural insights on nitrogen-containing hydrothermal carbon using solid-state magic angle spinning ^{13}C and ^{15}N Nuclear Magnetic Resonance. J. Phys. Chem. C 115, 8976-8982.

Bate-Smith, E.C., Swain, T., 1962.Flavonoid Compounds, in: Mason, H.S., Florkin, A.M. (Eds.), Comparative Biochemistry. Academic Press, New York, pp. 705-809.

Bimer, J., Salbut, P.D., Berlozecki, S., Boudou, J.P., Broniek, E., Siemieniewska, T., 1998. Modified active carbons from precursors enriched with nitrogen functions: sulphur removal capabilities. Fuel 77, 519–525.

Braghiroli, F.L., Fierro, V., Izquierdo, M.T., Parmentier, J., Pizzi, A., Celzard, A., 2012. Nitrogen-doped carbon materials produced from hydrothermally treated tannin. Carbon 50, 5411–5420.

Braghiroli, F., Fierro, V., Pizzi, A., Rode, K., Radke, W., Delmotte, L., Pizzi, A., Parmentier, J., Celzard, A., 2013. Reaction of condensed tannins with ammonia. Ind. Crop. Prod. 44, 330-335.

Braghiroli, F.L., Fierro, V., Izquierdo, M.T., Parmentier, J., Pizzi, A., Celzard, A., 2014. Kinetics of the hydrothermal treatment of tannin for producing carbonaceous microspheres. Bioresource Technol. 151, 271-277.

Brunauer, S., Emmet, P.H., Teller, E., 1938. Adsorption of gases in multimolecular layers. J. Am. Chem. Soc. 60, 309-319.

Cagniant, D., Magri, P., Gruber, R., Berlozecki, S., Salbut, P.D., Bimer, J., Nansé, G., 2002.Ammoxidation of cellulose - a structural study. J. Anal. Appl. Pyrol. 65, 1-23.

Dubinin, M.M., 1989. Fundamentals of the theory of adsorption in micropores of carbon adsorbents – characteristics of their adsorption properties and microporous structures. Carbon 27, 457-467.

Frackowiak, E., Lota, G., Machnikowski, J., Kierzek, K., Vix, C., Béguin, F., 2006. Optimisation of supercapacitors using carbons with controlled nanotexture and nitrogen content. Electrochim. Acta 51,2209-2214.

Gregg, S.J., Sing, K.S.W., 1991. Adsorption surface area and porosity. Academic Press, New York.

Grishechko, L.I., Amaral-Labat, G., Szczurek, A., Fierro, V., Kuznetsov, B.N., Pizzi, A., Celzard, A., 2013. New tannin – lignin aerogels. Ind. Crop. Prod. 41, 347-355.

Hashida, K., Makino, R., Ohara, S., 2009. Amination of pyrogallol nucleus of condensed tannins and related polyphenols by ammonia water treatment. Holzforschung 63, 319-326.

Hemingway, R.W., 1989. Structural Variations in Proanthocyanidins and Their Derivatives, in: Hemingway, R.W., Karchesy, J.J., Branham, S.J. (Eds.), Chemistry and Significance of Condensed Tannins. Plenum Press, New York, pp. 83-107.

Hulicova, D., Kodama, M., Hatori, H., 2006. Electrochemical performance of nitrogen-enriched carbons in aqueous and non-aqueous supercapacitors. Chem. Mater. 18, 2318-2326.

Hulicova-Jurcakova, D., Seredych, M., Lu, G.Q., Bandosz, T.J., 2009. Combined effect of nitrogen- and oxygen-containing functional groups of microporous activated carbon on its electrochemical performance in supercapacitors. Adv. Funct. Mater. 19, 438-447.

Lahaye, J., Nanse, G., Fioux, Ph., Bagreev, A., Broshnik, A., Strelko, V., 1999. Chemical transformation during the carbonisation in air and the pyrolysis under argon of a inylpyridine–divinylbenzene copolymer by X-ray photoelectron spectroscopy. Appl. Surf. Sci. 147, 153-174.

Lee, Y.H., Lee, Y.F., Chang, K.H., Hu, C.C., 2011. Synthesis of N-doped carbon nanosheets from collagen for electrochemical energy storage/conversion systems. Electrochem. Commun. 13, 50-53.

Li, K., Ling, L., Lu, C., Qiao, W., Liu, Z., Liu, L., Mochida, I., 2001. Catalytic removal SO_2 over ammonia-activated carbon fibers. Carbon 39, 1803–1808.

Li, M., Li, W., Liu, S., 2011. Hydrothermal synthesis, characterization, and KOH activation of carbon spheres from glucose. Carbohydr. Res. 346, 999-1004.

Morisada, S., Kim, Y.H., Ogata, T., Marutani, Y., Nakano, Y., 2011. Improved adsorption behaviors of amine-modified tannin gel for palladium and platinum ions in acidic chloride solutions. Ind. Eng. Chem. Res. 50, 1875–1880.

Nieto-Marquez, A., Espartero, I., Lazo, J.C., Romero, A., Valverde, J.L., 2009. Direct synthesis of carbon and nitrogen-carbon nanospheres from aromatic hydrocarbons. Chem. Eng. J. 153, 211-216.

Pels, J.R., Kapteijn, F., Moulijn, J.A., Zhu, Q., Thomas, K.M., 1995. Evolution of nitrogen functionalities in carbonaceous materials during pyrolysis. Carbon 33, 1641-1653.

Pizzi A., 1983. Tannin-based wood adhesives, in: Pizzi, A. (Ed.), Wood Adhesives: Chemistry and Technology. Marcel Dekker, New York, pp. 177-248.

Pizzi, A., 1994. Advanced wood adhesive technology. M. Dekker, New York.

Pizzi, A., Mittal, K.L., 2003. Handbook of Adhesive Technology. Marcel Dekker, Inc., New York.

Pizzi, A., 2008. Tannins: Major Sources, Properties and Applications, in: Belgacem,M.N., Gandini, A. (Eds.), Monomers, Polymers and Composites from Renewable Resources. Elsevier, Oxford, pp. 179-200.

Przepiórski, J., 2006. Enhanced adsorption of phenol from water by ammonia-treated activated carbon. J. Hazard. Mater. 135, 453–456.

Qiu, Y., Yu, J., Shi, T., Zhou, X., Bai, X., Huang, J.Y., 2011. Nitrogen-doped ultrathin carbon nanofibers derived from electrospinning: Large-scale production, unique structure, and application as electrocatalysts for oxygen reduction. J. Power Sources 196, 9862-9867.

Reddy, B.R., Eoff, L., Dalrymple, E.D., Black, K., Brown, D., Rietjens, M., Halliburton, A., 2003. Natural polymer-based cross-linker system for conformance gel systems.Soc. Petrol. Eng. J. 8, 99-106.

555 Steele, B.C.H., Heinzel, A., 2001. Materials for fuel-cell technologies. Nature 414, 345-352.
556 Titirici, M.M., 2013. Sustainable Carbon Materials from Hydrothermal Processes. Wiley,
557 London.
558 Wang, X., Liu, J., Xu, W., 2012. One-step hydrothermal preparation of amino-functionalized
559 carbon spheres at low temperature and their enhanced adsorption performance towards
560 Cr(VI) for water purification. Colloids Surf. A 415, 288-294.
561 White, R.J., Antonietti, M., Titirici, M.M., 2009. Naturally inspired nitrogen doped
562 porous carbon. J. Mater. Chem. 19, 8645-8650.
563 White, R.J., Yoshizawa, N., Antonietti, M., Titirici, M.M., 2011. A sustainable synthesis of
564 nitrogen-doped carbon aerogels. Green Chem. 13, 2428-2434.
565 Wohlgemuth, S.A., Vilela, F., Titirici M.M., Antonietti, M., 2012a. A one-pot hydrothermal
566 synthesis of tunable dual heteroatom-doped carbon microspheres. Green Chem. 14, 741-
567 749.
568 Wohlgemuth, S.A., White, R.J., Willinger, M.G., Titirici, M.M., Antonietti, M., 2012b. A one-
569 pot hydrothermal synthesis of sulfur and nitrogen doped carbon aerogels with enhanced
570 electrocatalytic activity in the oxygen reduction reaction. Green Chem. 14, 1515-1523.
571 Zhang, D., Hao, Y., Ma, Y., Feng, H., 2012. Hydrothermal synthesis of highly nitrogen-doped
572 carbon powder. Appl. Surf. Sci. 258, 2510-2514.
573 Zhao, L., Baccile, N., Gross, S., Zhang, Y., Wei, W., Sun, Y., Antonietti, M., Titirici, M.M.,
574 2010. Sustainable nitrogen-doped carbonaceous materials from biomass derivatives.
575 Carbon 48, 3778-3787.
576 Zhao, L., Li-Zhen, F., Zhou, M.Q., Guan, H., Qiao, S., Antonietti, M., Titirici, M.M., 2010.
577 Nitrogen- containing hydrothermal carbons with superior performance in
578 supercapacitors. Adv. Mater. 22, 5202-5206.
579
580

Captions of the figures

Fig. 1: The main flavonoid unit contained in Mimosa tannin: prorobinetinidin (above), and the two possible structures that are obtained after amination of Mimosa tannin (Braghiroli et al., 2013).

Fig. 2: Chemical species suggested from the analysis of MALDI-ToF spectra of hydrothermal aminated carbon gel before pyrolysis, H-EAT: (a) 554 Da; (b) 555 Da; (c) 843 Da (the sodium of weight 23 was implicitly taken into account).

Fig. 3: Nitrogen content of N-doped materials prepared by HTC at different temperatures, before and after pyrolysis before (H-T ◇, H-AT □ and H-EAT △), and after pyrolysis at 900°C (CH-T ◆, CH-AT■ and CH-EAT ▲).

Fig. 4:SEM images of tannin-based materials after HTC and posterior pyrolysis at 900°C: (a) CH-T_190°C and (b) CH-T_210°C; (c) CH-AT_190°C and (d) CH-AT_210°C; (e) CH-EAT_190°C and (f) CH-EAT_210°C.

Fig. 5: Surface areas, S_{BET}, of all materials obtained after HTC at different temperatures: before (H-T ◇, H-AT □ and H-EAT △), and after pyrolysis at 900°C (CH-T ◆, CH-AT ■ and CH-EAT ▲).

Fig. 6: Nitrogen adsorption (full symbols) – desorption (empty symbols) isothermsat -196°C. (CH-T_190°C ◆, CH-T_210°C ■; CH-AT_190°C ◆, CH-AT_210°C ■, CH-EAT_190°C ◆, CH-EAT_210°C ■).

Fig. 7: Nitrogen content vs. surface areas, S_{BET},of our materials: (a) before pyrolysis (H-T ◇, H-AT □ and H-EAT △); (b) after pyrolysis (CH-T ◆, CH-AT ■ and CH-EAT ▲) compared to results reported in literature.

High surface - highly N-doped carbons from hydrothermally-treated tannin

Braghiroli FL et al.

Table 1: Contributions to the N1s bands in XPS patterns of HTC samples.

	Binding energy (eV)	(at. %)		
	Isolated Pyridinic (N-6) and/ or Neutral amines	N_{XPS}	C_{XPS}	O_{XPS}
H-AT_180ºC	399.2	7.9	76.4	15.6
H-AT_190ºC	399.1	8.1	78.7	13.2
H-AT_210ºC	399.3	9.4	78.6	12.0
H-EAT_180ºC	399.1	2.5	76.6	18.3
H-EAT_190ºC	399.5	3.2	78.5	18.3
H-EAT_210ºC	399.3	3.4	78.2	18.4

High surface - highly N-doped carbons from hydrothermally-treated tannin

Braghiroli FL et al.

Table 2: Contributions to the N1s bands in XPS patterns of carbonised HTC samples.

	Binding energy (eV) and area of the peak (%)			(at. %)		
	Pyridinic (N-6)	Pyrrolic (N-5) or pyridonic	Quaternary N-Q or oxydised pyrinic N	N_{XPS}	C_{XPS}	O_{XPS}
CH-AT_180ºC	398.1 (35.7)	400.6 (55.3)	402.8 (9.0)	4.9	90.8	4.3
CH-AT_190ºC	398.1 (38.2)	400.7 (57.7)	402.7 (4.1)	2.8	92.4	4.8
CH-AT_210ºC	398.1 (39.2)	400.7 (59.2)	402.7 (1.6)	4.0	90.2	5.8
CH-EAT_180ºC	398.1 (33.1)	400.7 (60.1)	402.8 (6.8)	1.6	95.8	2.6
CH-EAT_190ºC	398.0 (36.7)	400.6 (60.9)	402.6 (2.4)	2.1	92.1	5.8
CH-EAT_210ºC	398.1 (37.1)	400.7 (61.2)	402.7 (1.7)	1.9	94.4	3.7

High surface - highly N-doped carbons from hydrothermally-treated tannin

Braghiroli FL et al.

Figure 1

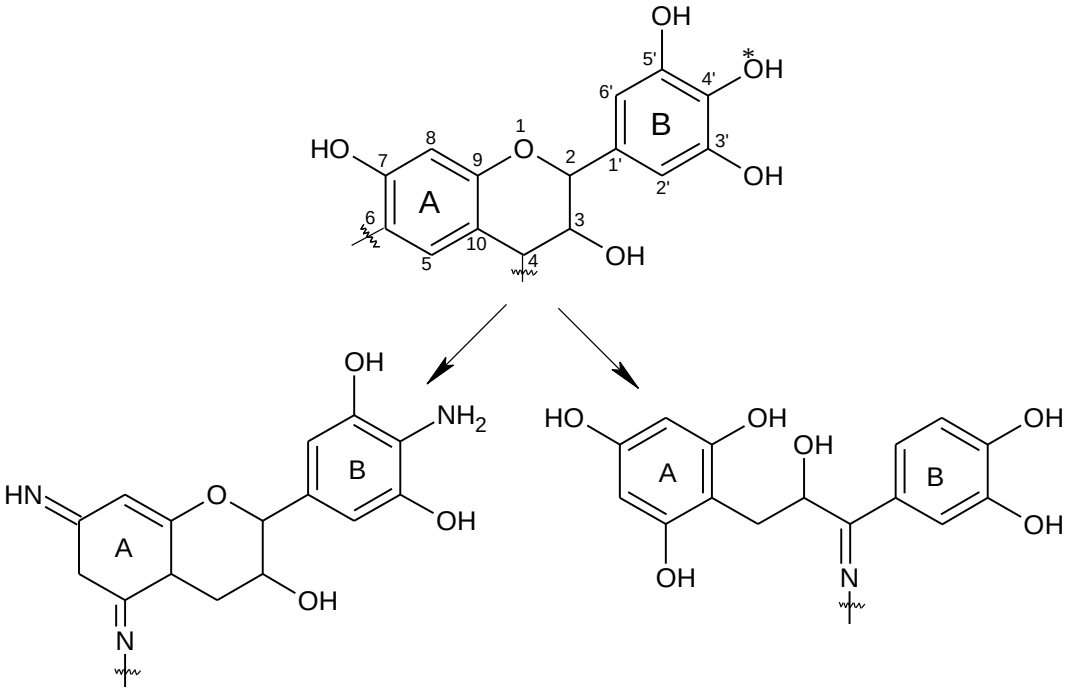

Fig. 1: The main flavonoid unit contained in Mimosa tannin: prorobinetinidin (above), and the two possible structures that are obtained after amination of Mimosa tannin (Braghiroli et al., 2013).

High surface - highly N-doped carbons from hydrothermally-treated tannin
Braghiroli FL et al.

Figure 2

(a)

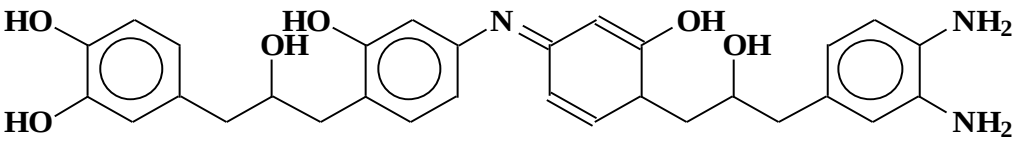

(b)

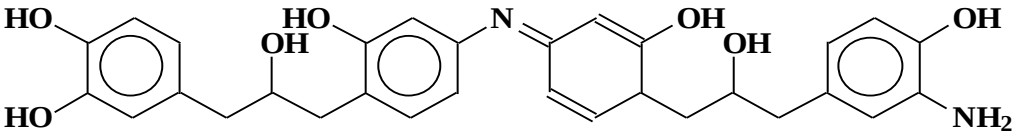

(c)

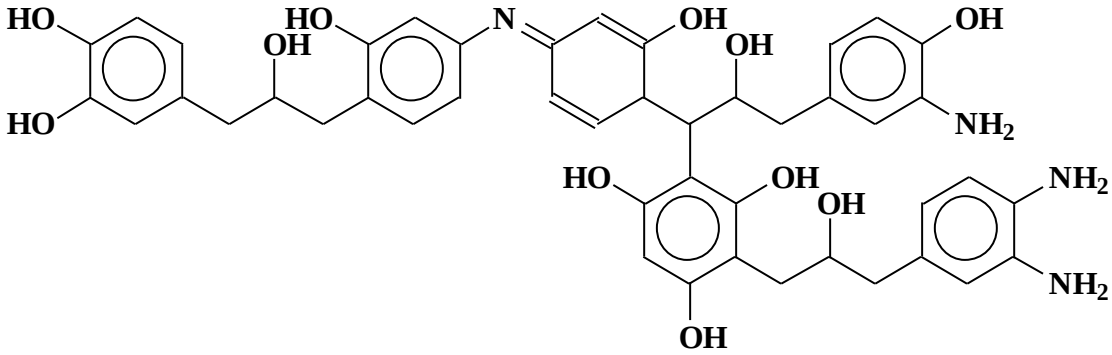

Fig. 2: Chemical species suggested from the analysis of MALDI-ToF spectra of hydrothermal aminated carbon gel before pyrolysis, H-EAT: (a) 554 Da; (b) 555 Da; (c) 843 Da (the sodium of weight 23 was implicitly taken into account).

High surface - highly N-doped carbons from hydrothermally-treated tannin

Braghiroli FL et al.

Figure 3

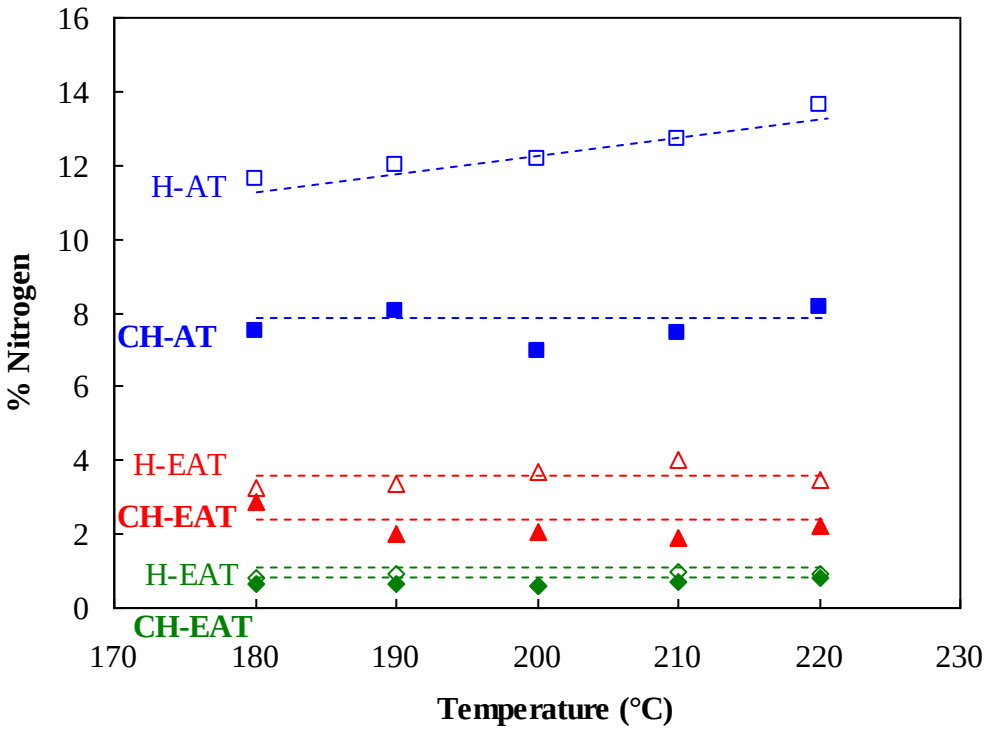

Fig. 3: Nitrogen content of N-doped materials prepared by HTC at different temperatures, before and after pyrolysis before (H-T ◇, H-AT □ and H-EAT △), and after pyrolysis at 900°C (CH-T ◆, CH-AT ■ and CH-EAT ▲).

High surface - highly N-doped carbons from hydrothermally-treated tannin

Braghiroli FL et al.

Figure 4

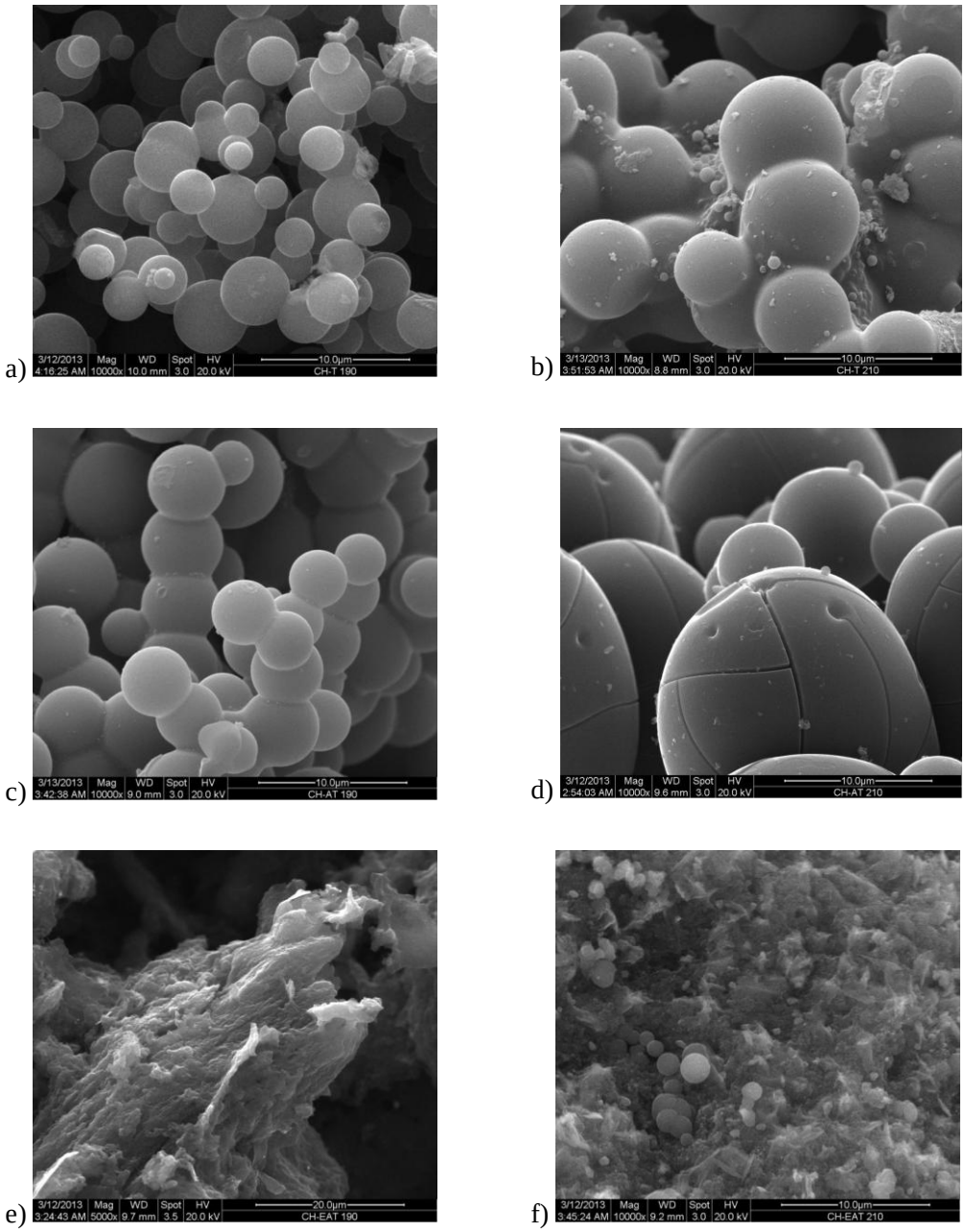

Fig. 4: SEM images of tannin-based materials after HTC and posterior pyrolysis at 900°C: (a) CH-T_190°C and (b) CH-T_210°C; (c) CH-AT_190°C and (d) CH-AT_210°C; (e) CH-EAT_190°C and (f) CH-EAT_210°C.

High surface - highly N-doped carbons from hydrothermally-treated tannin

Braghiroli FL et al.

Figure 5

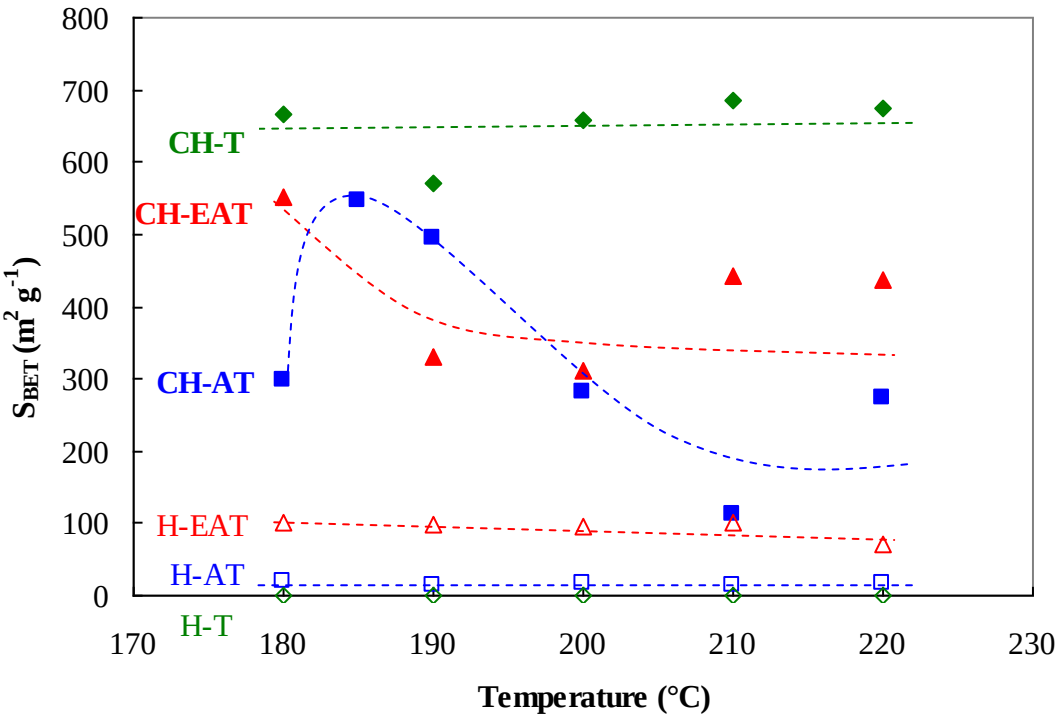

Fig. 5: Surface areas, S_{BET}, of all materials obtained after HTC at different temperatures: before (H-T ◇, H-AT □ and H-EAT △), and after pyrolysis at 900°C (CH-T ◆, CH-AT ■ and CH-EAT ▲).

High surface - highly N-doped carbons from hydrothermally-treated tannin

Braghiroli FL et al.

Figure 6

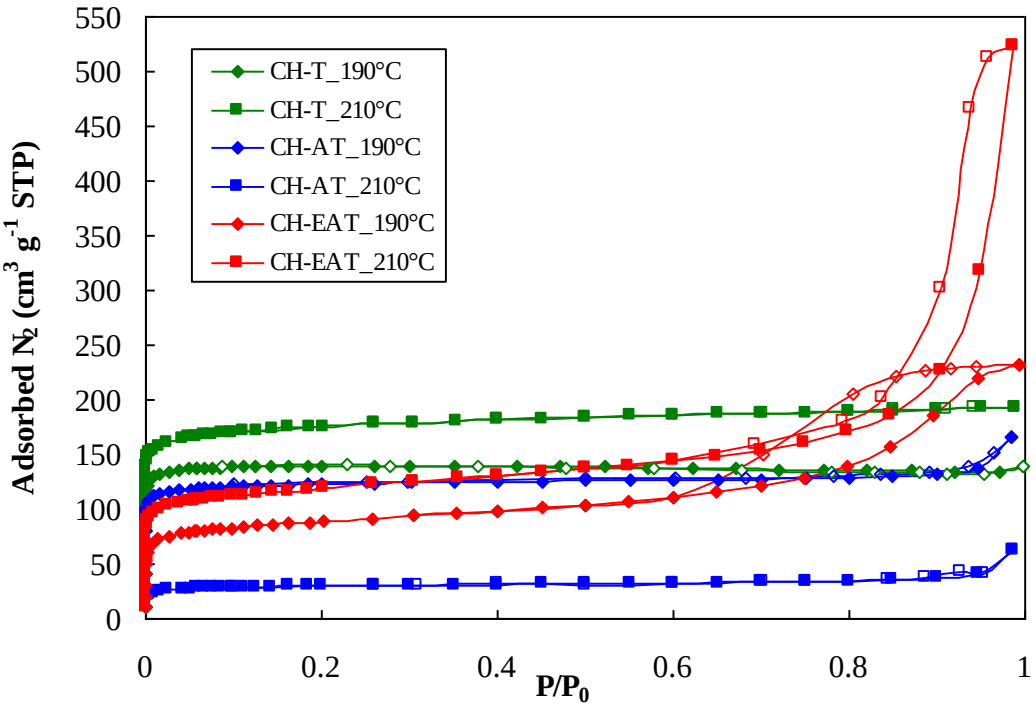

Fig. 6: Nitrogen adsorption (full symbols) – desorption (empty symbols) isotherms at -196°C. (CH-T_190°C ◆, CH-T_210°C ■; CH-AT_190°C ◆, CH-AT_210°C ■, CH-EAT_190°C ◆, CH-EAT_210°C ■).

High surface - highly N-doped carbons from hydrothermally-treated tannin

Braghiroli FL et al.

Figure 7

a)

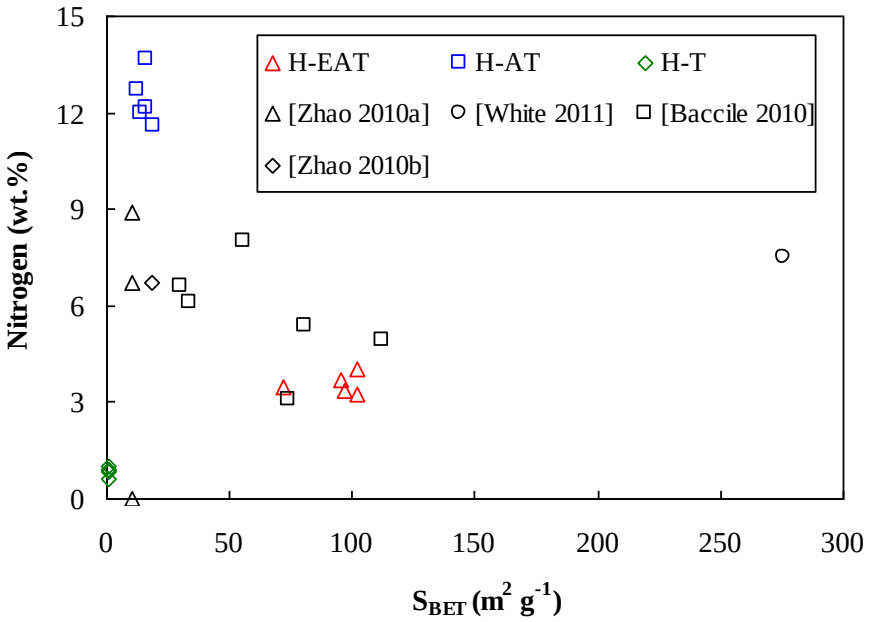

b)

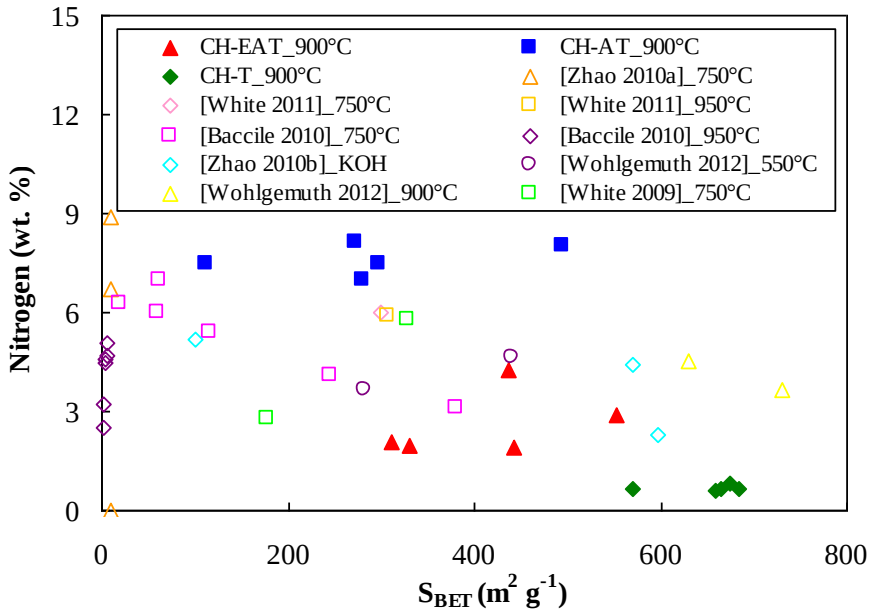

Fig. 7: Surface areas, S_{BET}, and nitrogen content of our materials: (a) before pyrolysis (H-T ◇, H-AT □ and H-EAT △); (b) after pyrolysis (CH-T ◆, CH-AT ■ and CH-EAT ▲) compared to results reported in literature.

e-component

Click here to download e-component: Supp material_HSHN_fbraghiroli-completed.docx